

Compact Printed Strip MIMO Antenna for 4G USB Dongle Applications

Minseok Han

*Department of Electronics Engineering
Osan University, Osan City, GyeongGi-Do, South Korea*

Abstract- A compact multiband MIMO antenna with an embedded chip inductor is proposed for 4th generation USB dongle applications. The proposed MIMO antenna consists of a longer strip with an embedded chip inductor and a shorter radiating strip. The longer radiating strip with a 15 nH embedded chip inductor has a length of only about 34 mm (about 0.08 wavelength at 0.77 GHz), but it supports a wide resonant mode for long term evolution band 13 (LTE Band 13; 0.746-0.787 GHz) and wireless broadband band (WiBro band; 2.3-2.4 GHz) services. The shorter radiating strip has a length of 12 mm (about 0.1 wavelength at 2.0 GHz) and provides a wide resonant mode at about 2 GHz for wideband code division multiple access band (WCDMA band; 1.92-2.17 GHz) operation. The two radiating strips occupy a small printed area of about 500 mm² on the system circuit board of a USB dongle. The proposed MIMO antenna has an isolation of approximately 17 dB at LTE band 13 and the envelope correlation coefficient (ECC) of the two antennas is less than 0.4 over the whole LTE band 13. To evaluate the performance of the proposed antenna, key performance parameters such as the total efficiency, ECC, mean effective gain (MEG), and the MEG ratio are analyzed.

Keywords – MIMO, isolation, chip inductor, multiband, LTE, USB dongle

I. INTRODUCTION

A multiple-input multiple-output (MIMO) technique has been considered as one of the most promising technologies for enhancing the performance of wireless communication systems with high-speed transmission rates. A MIMO system utilizing several antenna components is more advantageous than a single-input single-output (SISO) system in terms of increasing channel capacity and reducing transmitting power [1]. Conventional universal serial bus (USB) dongles are attractive for providing plug-and-play functionality in mobile communication devices such as laptops. Future wireless USB dongles should be capable of accommodating higher data rates than are current systems because of the development of various multimedia services. However, it is very challenging to place multiple antennas within small USB dongles while maintaining good isolation between the antenna elements since antennas can be strongly coupled with each other and even with the ground plane by sharing the surface currents distributed on the ground plane. So far, many investigations of multi-antenna systems using various techniques have been conducted with the goal of improving the isolation between the antenna elements. Mushroom-like electromagnetic band gap (EBG) structures can suppress the surface wave between antenna elements [2], and thus reduce the mutual coupling between the antenna elements. However, a number of mushroom-like structures must be placed under the antenna elements it requires an additional area. The defected ground structure (DGS) [3] or a simple ground plane modification [4] has also been shown to provide a band-stop effect by suppressing the ground current flowing between the antenna elements. However, these techniques cannot be utilized for a practical USB dongle with other electronic components when the solid ground plane printed circuit board (PCB) is modified or removed. In addition, a dual-polarization coplanar waveguide (CPW)-fed slot antenna was proposed in [5]. Since it is based on slot antenna, the size may not be suitable for very small USB dongle. In [6], two folded monopoles with a connecting line facing to the feed point are used to obtain the polarization and pattern diversity with excellent isolation characteristic. However, this approach can be used only for a single band application. The integration of compact printed multi-element antenna (MEA) systems operating in the 5.2 GHz Industrial, Scientific and Medical (ISM) band was proposed [7], but these systems are not applicable to our case.

In this paper, we propose a compact printed strip MIMO antenna with an embedded chip inductor for next generation USB dongle application. The proposed MIMO antenna consists of a longer radiating strip with an embedded chip inductor and a shorter radiating strip. The longer and shorter strips can be placed close to each other in order to form a compact structure. The embedded chip inductor contributes additional inductance that

compensates for the increased capacitance resulting from the shortened radiating strip. The designed multiband MIMO antenna has been successfully implemented, and the experimental results are presented and discussed

II. MIMO ANTENNA STRUCTURE AND DESIGN

The geometry of the proposed MIMO antenna embedded with a chip inductor for next generation USB dongle applications is shown in Fig. 1. Two of the same elements are placed at the two corners of the top edge of a 25 mm× 66 mm× 0.8 mm FR4 ($\epsilon_r = 4.4$), which simulates the ground plane of a practical USB dongle. The total printed area for two radiating elements is about 500 mm² on the system circuit board of a USB dongle. The basic structure of each radiating element is a simple two-strip planar inverted F antenna (PIFA). The shorter radiating strip has a length of about 12 mm, which is about 0.1 wavelengths at 2.0 GHz and can easily generate a wide resonant mode to cover WCDMA operation for the 2.05 GHz band. The longer strip with a 15 nH embedded chip inductor has a total length of about 34 mm, which is about 0.08 wavelength at 0.77 GHz, but it supports a wide resonant mode for LTE band 13 and WiBro band services. WiBro is the South Korean service name for IEEE 802.16e (mobile WiMAX) international standard. Owing to the embedded chip inductor, the resonant mode contributed by the longer strip can be effectively shifted to a lower frequency of about 0.77 GHz, from 1.3 GHz. A simulation was conducted using the commercially available simulation software MWS [8] in order to optimize the geometric parameters of the proposed antenna.

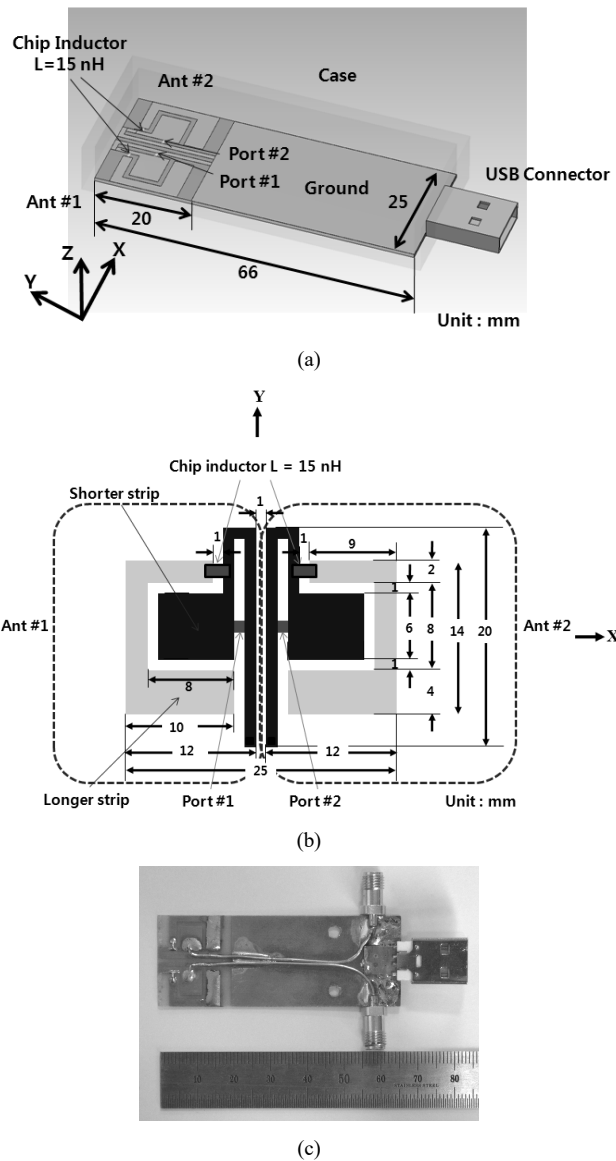


Figure 1. Geometry of the proposed compact MIMO antenna embedded with a chip inductor for next generation USB Dongle applications. Figure 2. (a) 3D view of the proposed MIMO antenna, (b) MIMO antenna structure, and (c) fabricated MIMO antenna.

Fig. 2 shows the simulated S-parameter characteristic of the proposed MIMO antenna with and without a chip inductor (longer strip and shorter strip are directly connected). It is evident that, because of the embedded chip inductor, the antenna's lower resonant frequency is shifted to a lower frequency, from about 1.2 GHz to 0.77 GHz for LTE band 13, and the isolation at LTE band 13 is higher than 18 dB. In our design, an embedded chip inductor as a series inductance is placed between the longer strip and shorter strip with 1 mm gap coupling. The loop structure formed by the shorting pin and feed line can be modeled as a shunt inductance. In addition, the distance between the shorting line of antenna #1 and the shorting line of antenna #2 is only 1 mm. Thus, this structure inherently plays a role of an effective band stop filter at LTE band 13. The total length of the loop structure formed by the shorting pin and the distance between the shorting line of antenna #1 and the shorting line of antenna #2 determine the inductance and capacitance, respectively.

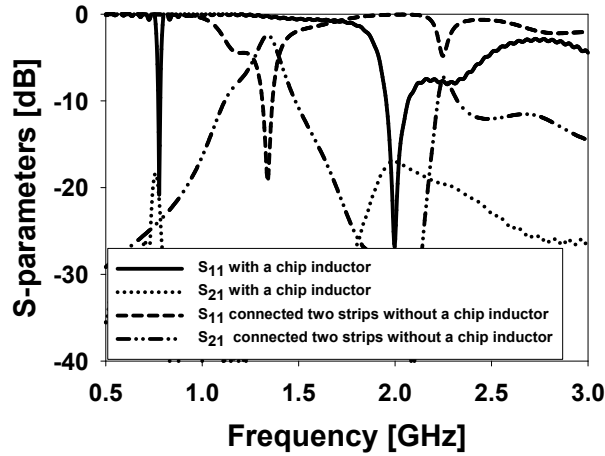


Figure 3. Simulated S-parameter characteristics of the proposed MIMO antenna with and without a chip inductor (longer strip and shorter strip are directly connected).

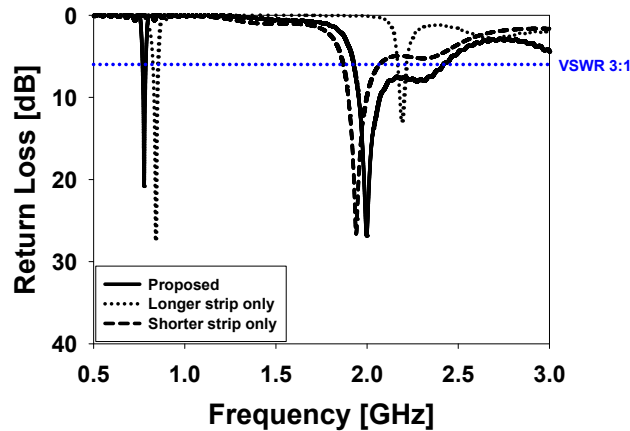


Fig. 3. Simulated return loss for the proposed MIMO antenna

Fig. 4 shows the effects of the inductance value of the embedded chip inductor on the antenna performances. The results indicate that the lower resonance frequency becomes lower as L increases. This behavior is reasonable, since a larger inductance can compensate for the larger capacitance resulting from the shortened length of the longer strip. The change in the upper band resonance frequency is minimal.

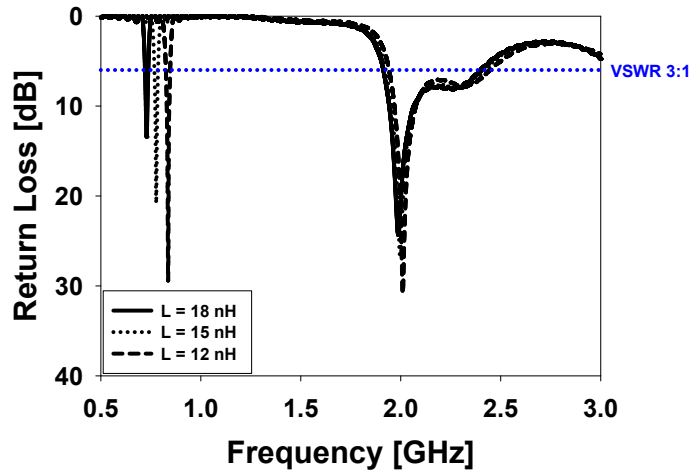


Fig. 4. Simulated return loss of the proposed MIMO antenna as a function of the inductance L of the embedded chip inductor.

III. EXPERIMENTAL RESULTS AND DISCUSSIONS

In order to validate the proposed MIMO antenna, an HP8719ES vector network analyzer was used to measure S-parameter characteristics of the fabricated MIMO antenna in an anechoic chamber. When we measure the antenna #1, port 1 is excited and port 2 is terminated by a 50 ohm load. Antenna #2 is measured in the same way.

Fig. 5 shows the measured S-parameter characteristics of the proposed MIMO antenna. From the measured results, the 6-dB return loss impedance bandwidth is 3.92% (from 750 MHz to 780 MHz) for LTE band 13, and the isolation at LTE band 13 is higher than 17 dB.

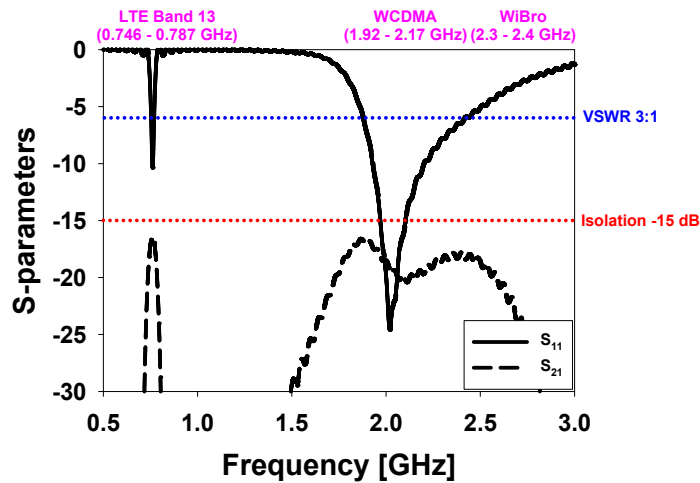


Fig. 5. Measured S-parameter characteristics

Fig. 6 shows the measured radiation patterns of the fabricated MIMO antenna (antenna #1) at 0.77, 2.05, and 2.35 GHz. When we measure the radiation patterns of antenna #1, port 1 is excited and port 2 is terminated by a 50 ohm load. In H (xz)-plane patterns, monopole-like radiation patterns are obtained at all three frequencies. The measured peak gains of the two antenna elements are -0.52 dBi and -0.64 dBi at the LTE band 13, 3.5 dBi and 2.9 dBi at the WCDMA band, and 3.4 dBi and 3.2 dBi at the WiBro band.

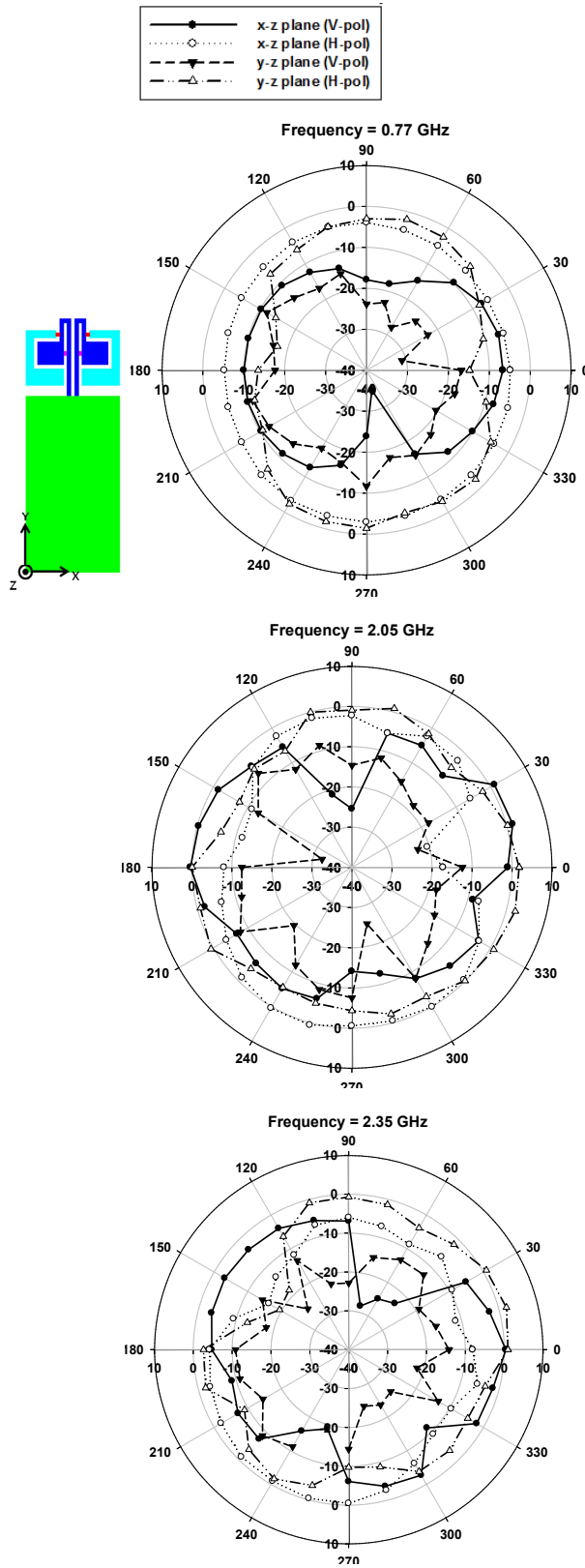


Fig. 6. Measured radiation patterns of the fabricated MIMO antenna (antenna #1)

IV. EVALUATION OF MIMO ANTENNA PERFORMANCE

To evaluate the performance of the proposed MIMO antenna, key performance parameters such as the ECC, MEG, and MEG ratio are analyzed. For diversity and MIMO applications, the correlation between the signals received by the involved antennas at the same side of a wireless link is an important figure of merit for the whole system. Usually, the ECC is used to evaluate the diversity capability of a multi-antenna system. This parameter should ideally be computed using the 3D radiation patterns [9], but this method is quite laborious. Assuming that the antennas are operating in a uniform multi-path environment ($XPR = 1$ and), antennas should have high efficiency and no mutual losses and load termination of the non-measured antenna is 50 ohms, the ECC can be alternatively calculated by using the scattering parameters. The ECC of two antennas is given by [10]

$$\rho_{12} = \frac{|S_{11}^* S_{12} + S_{12}^* S_{22}|^2}{(1 - |S_{11}|^2 - |S_{21}|^2)(1 - |S_{22}|^2 - |S_{12}|^2)} \quad (1)$$

Fig. 7 presents the ECC characteristics computed using the scattering parameters shown in Fig. 5. For $S_{21} > 10$ dB, the ECC values are maintained below 0.3. The ECCs of the two antennas are always lower than 0.4 over the whole frequency band. This leads us to expect good performance in terms of diversity [11].

$$\begin{aligned} MEG &= \frac{\text{mean received power}}{\text{total mean incident power}} \\ &= \int_0^{2\pi} \int_0^\pi \left(\frac{XPR}{1 + XPR} G_\theta(\theta, \phi) P_\theta(\theta, \phi) + \frac{1}{1 + XPR} G_\phi(\theta, \phi) P_\phi(\theta, \phi) \right) \sin \theta d\theta d\phi \end{aligned} \quad (2)$$

where P_θ and P_ϕ are the angular density functions of the incident power, and XPR represents the cross-polarization power ratio.

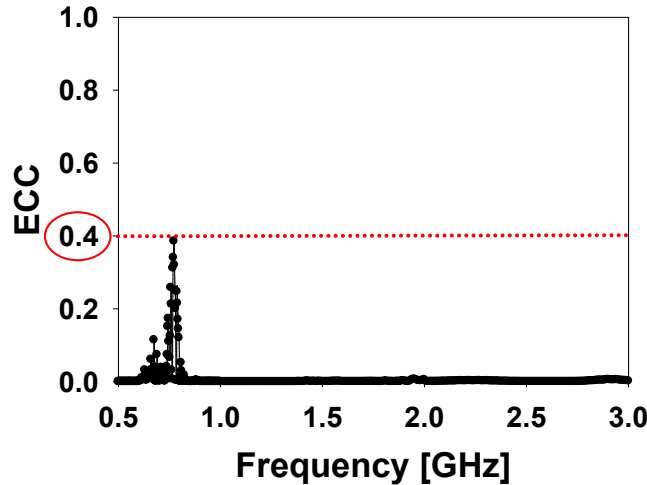


Fig. 7. Calculated ECC characteristics from measured S-parameters

In order to characterize the performance of a multichannel MIMO antenna, additional parameters such as the MEG and MEG ratio are often used. The MEG is a statistical measure of the antenna gain in a mobile environment and is equal to the ratio of the mean received power of the antenna to the total mean incident power. It can be expressed by equation (2) as defined in [11]: P_θ and P_ϕ are the θ - and ϕ -components of the angular density functions of incoming plane waves, respectively, from a statistical model in which the angular density functions are assumed to be Gaussian in elevation and uniform in the azimuth planes.

In the case of a uniform propagation environment in which $XPR = 1$ and $P_\theta = P_\phi = 1/4\pi$, the MEG is equal to the total antenna efficiency divided by two or -3 dB [7]. Moreover, to achieve a good diversity gain, the average received power from each antenna element must be nearly equal; this corresponds to a MEG ratio near unity.

The performance of the proposed MIMO antenna, including the total efficiency, MEG, and MEG ratio, is summarized in Table 1. From Table 1, it is found that the MEG for the two antenna elements are nearly equal demonstrated by the fact that the MEG ratio is close to unity [11].

$$10 \log |MEG_1/MEG_2| < 0.2 \text{ dB} \quad (3)$$

Table 1. Total efficiency, MEG and MEG ratio of the antennas

Frequency [GHz]	Total Efficiency [%]		MEG		MEG Ratio
	Antenna #1	Antenna #2	Antenna #1	Antenna #2	
0.77	28	29	14	14.5	0.96
2.05	56.8	56.2	28.4	28.1	1.01
2.35	53	53.6	26.5	26.8	0.98

IV. CONCLUSION

In this paper, a compact printed strip MIMO antenna with an embedded chip inductor for LTE/WCDMA/WiBro applications was proposed. The proposed MIMO antenna consists of a simple two-strip PIFA and embedded chip inductor. The antenna's lower and upper band resonances are contributed by the longer and shorter strips, respectively. The fabricated antenna has the isolation of about 17 dB at the lower band and higher than 20 dB at the higher band. The simulated and measured results show that the proposed multiband MIMO antenna could be a good candidate for the next generation USB Dongle applications.

V. REFERENCE

- [1] G. J. Foschini and M. J. Gans, "On limits of wireless communications in a fading environment when using multiple antennas," *Wireless Personal Comm.*, Vol. 6, No. 3, 311–335, Mar. 1998.
- [2] K. Payandehjoo and R. Abhari, "Employing EBG Structures in Multiantenna Systems for Improving Isolation and Diversity Gain", *IEEE Antennas and Wireless Propag. Lett.*, vol.8, pp.1162-1165, 2009.
- [3] F.-G. Zhu, J.-D. Xu and Q. Xu, "Reduction of mutual coupling between closely-packed antenna elements using defected ground structure", *IEEE Electronics Letters*, vol.45, no.12, pp.601-602, June, 2009.
- [4] A. C. K. Mak, C. R. Rowell, and R. D. Murch "Isolation enhancement between two closely packed antennas," *IEEE Transactions on Antennas and Propagation*, Vol.56, No.11, pp.3411-3419, Nov. 2008.
- [5] U. Li, Z. Zhang, W. Chen, Z. Feng and M. F. Iskander, "A Dual-Polarization Slot Antenna Using a Compact CPW Feeding Structure", *IEEE Antennas and Wireless Propag. Lett.*, vol.9, pp.191-194, 2009.
- [6] S. Park and C. Jung, "Compact MIMO antenna with high isolation performance", *IEEE Electronics Letters*, vol.46, no.6, pp.601-602, June, 2009.
- [7] M. P. Karaboikis, V. C. Papamichael, G. F. Tsachtsiris, C. F. Soras and V. T. Makios, "Integrating compact printed antennas onto small diversity/MIMO terminals," *IEEE Transactions on Antennas and Propagation*, vol. 56, no. 7, pp. 2067–2078, July. 2008.
- [8] Computer Simulation Technology (CST) Microwave Studio. Suite 2018 [Online]. Available: <http://www.cst.com>
- [9] I. Salonen and P. Vainikainen, "Estimation of signal correlation in antenna arrays," in *Proceedings of the 12th International Symposium Antennas (JINA '02)*, vol. 2, pp. 383-386, Nice, France, Nov. 2002.
- [10] S. Blanch, J. Romeu and I. Corbella, "Exact representation of antenna system diversity performance from input parameter description," *IEEE Electronics Letters*, vol.39, No. 9, May. 2003.
- [11] Taga, "Analysis for mean effective gain of mobile antennas in land mobile radio environments," *IEEE Trans. Veh. Technol.*, vol. 39, no. 2, pp.117-131, May. 1990.